

Nanowire Electrodes Integrated On Tip of Microwire for Peripheral Nerve Stimulation

Srinivasu Valagerahally Puttaswamy, Qiongfeng Shi, Aishwarya Bandla, Sangho Kim, Nitish V. Thakor and Chengkuo Lee

Srinivasu Valagerahally Puttaswamy and Prof. Sangho Kim

Department of Biomedical Engineering, National University of Singapore, 2 Engineering Drive 3, Singapore

Email: srini@nus.edu.sg

bieks@nus.edu.sg

Prof. Chengkuo Lee and Qiongfeng Shi

Singapore Institute for Neurotechnology (SINAPSE), National University of Singapore, 28 Medical Drive, #05-COR, Singapore 117456

Department of Electrical & Computer Engineering, National University of Singapore, 4 Engineering Drive 3, Singapore 117576

Center for intelligent sensors and MEMS (CSIM), National University of Singapore, Singapore

Graduate School for Integrative Science and Engineering, National University of Singapore, Singapore

Email: elelc@nus.edu.sg

qiongfeng@u.nus.edu

Prof. Nitish V. Thakor and Aishwarya Bandla

Singapore Institute for Neurotechnology (SINAPSE), National University of Singapore, 28 Medical Drive, #05-COR, Singapore 117456

Department of Biomedical Engineering, National University of Singapore, 2 Engineering Drive 3, Singapore

Department of Biomedical Engineering, School of Medicine, Johns Hopkins University Baltimore, MD 21205, USA

Email: sinapsedirector@gmail.com

aishwarya.bandla@nus.edu.sg

Abstract-Electrodes play a significant role in monitoring and inducing electrical activity in neural tissues. Electrode-nerve interface is engineered by employing zinc oxide nanowire electrodes which greatly increase contact area and coated with iridium oxide for low impedance. The work reported here provides a good platform for the development of an electrode system for chronic neural stimulation applications.

Index Terms-Nanowire, Electroceuticals, Nanoelectrodes, Nerve stimulation

Nanostructured electrodes are considered as a favorable substitute to conventional surface electrodes for neural interfaces, as they are penetrative, tissue-friendly and bio-stable to provide good coupling with the target neural tissues. Recent advances in the field of functional electrical stimulation has seen development in electrode fabrication technology, enabling applications such as prosthesis, rehabilitation, bladder control and sensory feedback. Such emerging electrode technologies of fabrication and interfacing of nanoelectrodes enables stimulation and recording of peripheral nerve action potentials [1]. An interest in peripheral nerve recording and stimulation with enhanced selectivity has led to the development of various designs in neural interfacing electrodes. Neural interfacing electrodes can be broadly classified into invasive or penetrating electrodes and non-invasive or surface sheet electrodes. Penetrating electrodes have been extensively used in stimulation and recording of nerve potentials. Various types of microelectrodes have been developed as penetrating electrodes both for cortical and nerve interface [2-6]. Microwires are one of the earliest types of penetrating electrodes which usually are comprised of thin wires made of stainless steel, tungsten and platinum/iridium, insulated to only expose the tip [7]. On the other hand, planar or non-invasive microelectrodes are designed to be flexible, soft and conveniently interfaced with neural tissues, without contributing to nerve tissue damage. These planar microelectrodes are thin-film electrode arrays embedded in flexible polymeric substrates [8] such as polydimethylsiloxane (PDMS) [9], polyimide [10-11] or parylene [12]. Most of the commercial electrodes are surface electrodes and they have been successfully employed for neurostimulation. However, they have limitations of resolution, specificity, poor contact with neural tissue to deliver sufficient current to stimulate. Nanowire (NW) electrodes may be a promising complement to conventional silicon based microelectrodes. Conventional silicon microprobes, with metal contacts of gold, lack the suitable impedance properties and may, for some applications, be too large. Coating them with carbon nanotubes is one way to improve the impedance of the electrodes.

Smaller and denser electrode arrays are the need of the hour to precisely, selectively stimulate and to record neural circuit activity. The electrode number and size should match the cells in the neural tissue. Nano sized electrodes provide many favorable advantages such as minimum cell-to-electrode distance and better resolution [13] enhanced electrical properties [14] and biocompatibility [15]. Recently different nanofabrication techniques have been used to create NWs for neural stimulation and recording. Nanoelectrodes have been grown epitaxially for cortical stimulation [16], with stamping and printing method [17], gallium phosphide NWs for acute *in vivo* recording in rat cortex [18]. Further, Nanowires were grown using electron-beam-induced deposition for recording neural signals in the rat brain [19] and silicon-based intracellular electrodes have been developed for neural recording [20].

Zinc oxide (ZnO) is a promising alternative material for NW electrodes as dense arrays of ZnO NWs could improve current density by providing direct conduction pathways.[21-22]. Current density refers to the amount of current being delivered to a specific area. A single large electrode will decrease current density whereas; electrodes of nano size with smaller surface area, will significantly improve current density for a given applied current. The nanowire electrodes also provide close contact and effective electrode–cell electrical coupling. The distinctive feature of ZnO is that with proper coating or doping, it can be made electrically conductive. Previous work on cellular level biocompatibility of ZnO NWs , report that ZnO NWs are completely biocompatible, biosafe, reliable and trustworthy for biomedical applications. The interaction of ZnO NWs with Hela cells was also methodically investigated through cell reproduction and growth assessment [23].

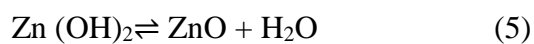
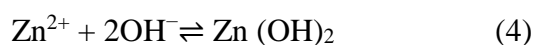
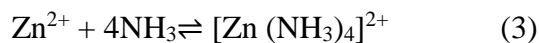
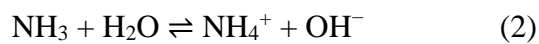
ZnO NWs, have been previously employed for various applications such as solar cells [24], photoelectrochemical process enhancement [25], strain sensors [26], lasers [27] and biosensing [28]. In this study, for the first time, we apply ZnO NWs for nerve stimulation application. For commercial applications of ZnO NWs, several approaches are employed for fabrication, such as thermal evaporation process [29], ultraviolet decomposition process [30], laser-assisted technique [31] and metal organic chemical vapour deposition [32]. Here, we employed the hydrothermal method which is comparatively a

low-temperature process producing high-quality single crystalline ZnO NWs [33]. ZnO nanostructures offer grain boundary and mostly defect-free single crystalline nature over their bulk counterparts, which could be beneficial for neural stimulation applications. Current nanoelectrode designs have limitations such as low aspect ratios or large substrates and thus are not suitable for stimulating especially small nerves.

The characteristics of a suitable invasive electrode include precise positioning in chronic implants, firm nerve-electrode contact and insulation to increase the current density. Moreover, the firm electrode contact with the nerve should be achieved without causing tissue damage. Suturing technique is employed to ensure strong electrode contact during stimulation and recording. However, this method is time consuming and potentially contributes to local tissue damage, thus rendering it unsuitable for chronic applications [34]. Hence, to resolve the issue of nerve electrode interfacing we have used photosensitive hydrogel, poly (ethylene glycol) diacrylate (PEGDA), as a biocompatible glue to secure the electrodes in position and to insulate from bodily fluids. Use of PEGDA is a simple, effective, non-invasive method, providing an immediate waterproof seal. The proposed adhesive is gradually metabolized and will not cause adverse effects on tissues, also preventing tissue deformation [35]. Glues which are currently available are expensive, have low adhesion strength [36] and are toxic. Thus, there is a strong need to employ a material with all the above-mentioned characteristics. In this work, electrode-nerve interface is engineered by employing platinum iridium microwire electrode, fabricated with ZnO NWs at the tip, coated with iridium oxide (IrOx) which increases contact area with reduced impedance. The results were tested in an *in vivo* application of a neural interface to the peripheral nerve. This demonstration of the use of PEGDA as an adhesive/insulating medium for neural interface applications has opened the possibility of extending scope to other *in vivo* applications requiring biocompatible adhesives.

Fig. 1(a-g) shows the fabrication steps of nanoelectrodes. ZnO NWs were fabricated via a simple, low temperature and low cost hydrothermal method, consisting of a seeding step followed by a growth step. All chemicals were purchased from Sigma-Aldrich and used without further purification. Before the

seeding step, platinum iridium microwires were first ultrasonically cleaned, in consecutive acetone (99.8%), isopropanol (99.8%) and deionized (DI) water baths for 10 minutes (Fig. 1(a)). Substrates were then dried with nitrogen gas. A low temperature pulse laser deposition (PLD) was used to deposit a thin ZnO layer (100 nm) on the substrate as seed layer for hydrothermal ZnO NWs growth (Fig. 1(b)).



The ZnO NWs growth process follow five chemical reactions listed above. All these reactions can be controlled through reaction parameters, such as precursor concentration, growth temperature and growth time, in order to push the reaction equilibrium forward or backward, which in turn allow us to tune length, diameter, aspect ratio and density of the ZnO NWs. NW density and aspect ratio is determined by precursor/growth solution concentration, growth time and temperature.

The seeded substrate was immersed into the growth solution, which contains 0.02 M zinc acetate dehydrate (ZAD) and 0.02 M hexamethylenetetramine (HMTA) (Fig. 1(c)). During the process, the growth solution was maintained at 90 °C in a conventional oven (Fig. 1(d)). After 6, 12, 18 and 24 hours, the substrate was taken out of the solution, rinsed with DI water to remove any residual salts and organic material and finally dried with nitrogen gas (Fig. 1(e-f)). For the support structure, initially we chose silicon substrate to optimize growth conditions and in the final stage, after growth parameters were optimized to grow NWs of required density and length, platinum iridium microwire of 75 µm diameter (20 µm at the tip, made of 90% platinum/10% iridium and insulated with polyimide; from California Fine Wire, CA, USA) was used. Similar protocol was followed to grow ZnO NWs at the tip of platinum iridium microwire as elucidated in Fig. 1(g). The variation of NW length with reaction time is depicted in

Fig. 2 (a, b). It can be observed from the figure that the length of ZnO NW increases linearly with growth time, after period of 6, 12, 18 and 24 hours. We used 12 hours of growth conditions for growing NW at the tip of platinum iridium microwire, as the aspect ratio and density of was suitable for our application. The surface morphology of the grown ZnO NWs on the tip of platinum iridium microwire employed with this growth condition is shown in Fig. 2 (c). From the SEM image of the samples, one can see that rod-like NWs have been fabricated at the tip of platinum iridium microwire, and the area density of the NWs was about $6.62 \times 10^8 / \text{cm}^2$. Well-aligned NWs grown vertically on the tip of the microwire are visible from the image, and the size of the NWs tapers from around 50 to 250 nm at the bottom to less than 30 to 150 nm at the top. The length of the NWs with growth time of 12 hours was about 4.75 μm . The aspect ratio of the NW was about 19 to 95. The fabricated NWs at the tip of the microwire were coated with IrOx films formed by electrodeposition [37] as a low impedance, high charge capacity coating for neural stimulation. The IrOx was directly deposited on the nanowire part, from an iridium salt solution and did not require activation of metal. The thickness of IrOx film was approximately 100 nm. The output impedance was recorded with an impedance analyzer (Zennium E, ZAHNER electric Inc, Germany). The impedance and phase angle at 1 kHz were 1 k Ω and -22°, respectively. The charge storage capacity (CSC) after iridium oxide coating was measured to be 26.59 mC/cm².

The experiments were performed in adult female Sprague Dawley rats (250 g) (In Vivos Pte Ltd, Singapore). The rats were acclimatized for one week prior to use in the experiment, with food and water provided *ad libitum* and 12 hours lights on/off cycle. The animal care and use procedures conformed to those outlined by the Agri-Food & Veterinary Authority of Singapore (AVA), the Institutional Animal Care and Use Committee (IACUC), and the ethics commission of the National University of Singapore. The animals were anesthetized with a single bolus injection of ketamine/xylazine (150 mg/kg and 10 mg/kg, respectively, intraperitoneal). After an adequate depth of anesthesia was attained, the right sciatic nerves were exposed through a gluteal-splitting incision. The ZnO nanowires electrodes penetrated sciatic nerve and were immediately covered and cured with PEGDA upon UV exposure. Special care was taken

to prevent nerve damage. The compound muscle action potentials (CMAPs) were recorded from the biceps femoris muscles with inhouse stainless steel wire electrodes. Fig. 3 (a-c) shows the schematic diagram illustrating electrode placement, insertion, insulation and corresponding microscopic images respectively. The reference electrode was placed in the body in an electrically neutral place. Ground electrode was separately connected to the tail of the rat. Electrophysiological data was analysed using custom-made algorithms in Matlab (Mathworks, Inc. USA).

The neural signals are evoked due to electrical stimulation by ZnO NW bipolar electrode during acute recording tests (studies done under general anesthesia); evoked activity is used for measuring CMAPs. In this study, a sciatic nerve was directly stimulated and the evoked CMAPs were recorded from the biceps femoris muscles with in-house stainless steel wire electrodes. The nerve was stimulated by the application 20 μ s pulse, with amplitudes varying between 60–160 μ A, using an isolated stimulator box (Digitimer Ltd., UK). We observed that electrical stimulation of rat sciatic nerve fibers delivered via ZnO nano electrodes could evoke hind limb muscle twitches. Signals from the implanted inhouse stainless steel electrodes were acquired using a multichannel amplifier (USB-ME32-FAI System, Multichannel Systems, Inc, USA), at a sampling rate of 50 kHz and a gain of 2000. Data acquisition was done using MCS system and the data acquisition software (MC Rack). The electrode body was embedded in PEGDA which is flexible and biocompatible, and only the tip was exposed, to prevent tissue inflammation. PEGDA was in contact with the body and prevented friction between tissue and stiff electrode material. The main advantage of the use of penetrating nanoelectrodes is that less current is needed to stimulate nerve fibers once the tips are inside the fascicle.

The recorded EMG signals under amplitudes varying between 60–160 μ A stimulation from ZnO NW bipolar electrode, recorded from biceps femoris muscles are shown in Fig. 4. The single neural activity recorded when stimulated at 60 μ A intensity with all traces and mean trace is shown in Fig. 4 (a). The mean EMG amplitude was 491.7 μ V at stimulation amplitudes of 60 μ A which was significantly high. The neural activity recorded with increasing stimulus intensity (from 60–160 μ A) is shown in Fig. 4 (b).

The evoked CMAPs are the algebraic summation of all the action potentials produced by all the fascicles within the nerve bundles excited by the electrical stimulation. When the stimulus current increased in steps of 20 μA from 60–160 μA , more fascicles were recruited and EMG signals increased progressively as represented in Fig. 4 (c). On the other hand, the time at which CMAPs reaches peak value reduced gradually when stimulus current is increased from 60–160 μA in steps of 20 μA as depicted in Fig. 4 (d). More action potentials added up to produce higher amplitude signals at 160 μA . Nevertheless, when the stimulus current increased to 180 μA , we observed movement of abdominal muscle as the current intensity was quite high and spread more widely and affected the tissue further from the stimulation site. On the other hand, when the stimulation current of the similar range (60–160 μA) was applied with conventional bare platinum iridium microwire electrodes without nanowire electrodes, only few fascicles were activated and muscle electrodes could not record any EMG signals.

In addition, we have employed photosensitive PEGDA hydrogel, which can be cured within few seconds to hold electrodes in position when interfaced with small nerves and it also functions as an insulating medium to prevent current leakage. Light-curing method employed by us has also the added benefit of reducing the processing costs, producing higher quality products, and eliminating the use of harmful chemicals from the workplace. This method can be conveniently applied to secure electrodes, even with small nerves. In contrast, other methods that pinch the nerve tightly may cause nerve injury. To validate this idea, we have employed PEGDA to secure different electrodes on both large and small nerve such as sciatic and vagus nerve and *in vivo* impedance was measured using Intan 2216 chip at 1 kHz frequency before and after the application of PEGDA. During application, PEGDA mixed with photoinitiator at low concentration applied over the electrode, cured with portable UV exposure equipment for 30 seconds to form a thin film. Soon after curing, *in vivo* impedance was measured at 1 kHz frequency. The impedance and phase angle at 1 kHz were 3 k Ω and -10° , respectively. In the current work, we employed PEGDA for acute *in vivo* test. However, similar approach could be employed for chronic application by intentionally introducing network defects in the hydrogel, resulting in the

formation of soft hydrogels with longer degradation times [38]. The network defects decouple degradation rate and mechanical properties of cross-linked hydrogel. The methods of employing PEGDA enable us to fix electrodes in position in a short span of time, compared to commercially available glues.

For the first time, in this work, we have demonstrated the application of ZnO nanoelectrodes for peripheral nerve stimulation, experimentally validated in a rodent model. A combination of NW electrode and PEGDA insulating cover to prevent current leakage resulting in passive transducers for direct communication with the neural tissues was demonstrated. Low-stimulus intensity resulted in large evoked CMAPs due to increased electrode active surface area by growing nanostructured materials and hydrogel insulation. Our results showed that such a delicate architecture of nanowire electrodes could be fabricated consistently for neural interface applications. The proposed method has potential applications in neuroprosthetics and in basic physiology research and provides a good platform for the development of interfascicular electrode system for chronic neural stimulation applications.

Acknowledgements

This work was supported by grants from the National Research Foundation (NRF) CRP project ‘Peripheral Nerve Prostheses: A Paradigm Shift in Restoring Dexterous Limb Function (NRF-CRP10-2012-01)’ (R-719-000-001-281)

References:

- [1] K. Famm, B. Litt, K. J. Tracey *et al.*, “Drug discovery: a jump-start for electroceuticals,” *nature*, vol. 496, no. 7444, pp. 159-161, 2013.
- [2] D. R. Kipke, R. J. Vetter, J. C. Williams *et al.*, “Silicon-substrate intracortical microelectrode arrays for long-term recording of neuronal spike activity in cerebral cortex,” *IEEE transactions on neural systems and rehabilitation engineering*, vol. 11, no. 2, pp. 151-155, 2003.
- [3] T. D. Y. Kozai, N. B. Langhals, P. R. Patel *et al.*, “Ultrasmall implantable composite microelectrodes with bioactive surfaces for chronic neural interfaces,” *Nature materials*, vol. 11, no. 12, pp. 1065-1073, 2012.
- [4] N. Lago, K. Yoshida, K. P. Koch *et al.*, “Assessment of biocompatibility of chronically implanted polyimide and platinum intrafascicular electrodes,” *IEEE Transactions on Biomedical Engineering*, vol. 54, no. 2, pp. 281-290, 2007.
- [5] C. T. Nordhausen, E. M. Maynard, and R. A. Normann, “Single unit recording capabilities of a 100 microelectrode array,” *Brain research*, vol. 726, no. 1, pp. 129-140, 1996.
- [6] T. Boretius, J. Badia, A. Pascual-Font *et al.*, “A transverse intrafascicular multichannel electrode (TIME) to interface with the peripheral nerve,” *Biosensors and Bioelectronics*, vol. 26, no. 1, pp. 62-69, 2010.
- [7] G. Lehew, and M. A. Nicolelis, “State-of-the-art microwire array design for chronic neural recordings in behaving animals,” *Methods for neural ensemble recordings*, vol. 2, pp. 361-371, 2008.
- [8] C. Hassler, T. Boretius, and T. Stieglitz, “Polymers for neural implants,” *Journal of Polymer Science Part B: Polymer Physics*, vol. 49, no. 1, pp. 18-33, 2011.
- [9] S. P. Lacour, S. Benmerah, E. Tarte *et al.*, “Flexible and stretchable micro-electrodes for in vitro and in vivo neural interfaces,” *Medical & biological engineering & computing*, vol. 48, no. 10, pp. 945-954, 2010.

- [10] B. Rubehn, C. Bosman, R. Oostenveld *et al.*, “A MEMS-based flexible multichannel ECoG-electrode array,” *Journal of neural engineering*, vol. 6, no. 3, pp. 036003, 2009.
- [11] S. Myllymaa, K. Myllymaa, H. Korhonen *et al.*, “Fabrication and testing of polyimide-based microelectrode arrays for cortical mapping of evoked potentials,” *Biosensors and Bioelectronics*, vol. 24, no. 10, pp. 3067-3072, 2009.
- [12] H. Toda, T. Suzuki, H. Sawahata *et al.*, “Simultaneous recording of ECoG and intracortical neuronal activity using a flexible multichannel electrode-mesh in visual cortex,” *Neuroimage*, vol. 54, no. 1, pp. 203-212, 2011.
- [13] C. Xie, Z. Lin, L. Hanson, Y. Cui, and B. Cui, “Intracellular recording of action potentials by nanopillar electroporation,” *Nat Nano*, vol. 7, no. 3, pp. 185-190, 2012.
- [14] A. Ansaldo, E. Castagnola, E. Maggiolini, L. Fadiga, and D. Ricci, “Superior Electrochemical Performance of Carbon Nanotubes Directly Grown on Sharp Microelectrodes,” *ACS Nano*, vol. 5, no. 3, pp. 2206-2214, 2011.
- [15] T. Berthing, S. Bonde, C. B. Sørensen, P. Utko, J. Nygård, and K. L. Martinez, “Intact Mammalian Cell Function on Semiconductor Nanowire Arrays: New Perspectives for Cell-Based Biosensing,” *Small*, vol. 7, no. 5, pp. 640-647, 2011.
- [16] L. Gällentoft, L. M. E. Pettersson, N. Danielsen, J. Schouenborg, C. N. Prinz, and C. E. Linsmeier, “Size-dependent long-term tissue response to biostable nanowires in the brain,” *Biomaterials*, vol. 42, pp. 172-183, 2015.
- [17] I. von Ahnen, G. Piret, and C. N. Prinz, “Transfer of vertical nanowire arrays on polycaprolactone substrates for biological applications,” *Microelectronic Engineering*, vol. 135, pp. 52-56, 2015.
- [18] D. B. Suyatin, L. Wallman, J. Thelin, C. N. Prinz, H. Jörntell, L. Samuelson, L. Montelius, and J. Schouenborg, “Nanowire-Based Electrode for Acute In Vivo Neural Recordings in the Brain,” *PLOS ONE*, vol. 8, no. 2, pp. e56673, 2013.

- [19] J. E. Ferguson, C. Boldt, J. G. Puhl, T. W. Stigen, J. C. Jackson, K. M. Crisp, K. A. Mesce, T. I. Netoff, and A. D. Redish, "Nanowires precisely grown on the ends of microwire electrodes permit the recording of intracellular action potentials within deeper neural structures," *Nanomedicine (London, England)*, vol. 7, no. 6, pp. 847-853, 2012.
- [20] J. Robinson, M. Jorgolli, and H. Park, "Nanowire electrodes for high-density stimulation and measurement of neural circuits," *Frontiers in Neural Circuits*, vol. 7, no. 38, pp. 1-5, 2013.
- [21] W. L. Ong, C. Zhang, and G. W. Ho, "Ammonia plasma modification towards a rapid and low temperature approach for tuning electrical conductivity of ZnO nanowires on flexible substrates," *Nanoscale*, vol. 3, no. 10, pp. 4206-4214, 2011.
- [22] S. Minne, S. Manalis, and C. Quate, "Parallel atomic force microscopy using cantilevers with integrated piezoresistive sensors and integrated piezoelectric actuators," *Applied Physics Letters*, vol. 67, no. 26, pp. 3918-3920, 1995.
- [23] Z. Li, R. Yang, M. Yu, F. Bai, C. Li, and Z. L. Wang, "Cellular Level Biocompatibility and Biosafety of ZnO Nanowires," *The Journal of Physical Chemistry C*, vol. 112, no. 51, pp. 20114-20117, 2008.
- [24] Q. Zhang, S. Yodyingyong, J. Xi *et al.*, "Oxide nanowires for solar cell applications," *Nanoscale*, vol. 4, no. 5, pp. 1436-1445, 2012.
- [25] T. Wang, Z. Jiao, T. Chen *et al.*, "Vertically aligned ZnO nanowire arrays tip-grafted with silver nanoparticles for photoelectrochemical applications," *Nanoscale*, vol. 5, no. 16, pp. 7552-7557, 2013.
- [26] Q. Liao, M. Mohr, X. Zhang *et al.*, "Carbon fiber-ZnO nanowire hybrid structures for flexible and adaptable strain sensors," *Nanoscale*, vol. 5, no. 24, pp. 12350-12355, 2013.
- [27] D. Vanmaekelbergh, and L. K. Van Vugt, "ZnO nanowire lasers," *Nanoscale*, vol. 3, no. 7, pp. 2783-2800, 2011.

- [28] J. Lee, S. Choi, S. J. Bae *et al.*, “Visible light-sensitive APTES-bound ZnO nanowire toward a potent nanoinjector sensing biomolecules in a living cell,” *Nanoscale*, vol. 5, no. 21, pp. 10275-10282, 2013.
- [29] M. C. McAlpine, R. S. Friedman, and C. M. Lieber, “High-performance nanowire electronics and photonics and nanoscale patterning on flexible plastic substrates,” *Proceedings of the IEEE*, vol. 93, no. 7, pp. 1357-1363, 2005.
- [30] J. M. Wu, Y.-R. Chen, and Y.-H. Lin, “Rapidly synthesized ZnO nanowires by ultraviolet decomposition process in ambient air for flexible photodetector,” *Nanoscale*, vol. 3, no. 3, pp. 1053-1058, 2011.
- [31] C. Fauteux, R. Longtin, J. Pegna *et al.*, “Fast synthesis of ZnO nanostructures by laser-induced decomposition of zinc acetylacetonate,” *Inorganic chemistry*, vol. 46, no. 26, pp. 11036-11047, 2007.
- [32] J.-J. Wu, and S.-C. Liu, “Low-temperature growth of well-aligned ZnO nanorods by chemical vapor deposition,” *Advanced Materials*, vol. 14, no. 3, pp. 215, 2002.
- [33] S. Zhang, Y. Shen, H. Fang *et al.*, “Growth and replication of ordered ZnO nanowire arrays on general flexible substrates,” *Journal of Materials Chemistry*, vol. 20, no. 47, pp. 10606-10610, 2010.
- [34] A. Narakas, “The use of fibrin glue in repair of peripheral nerves,” *The Orthopedic clinics of North America*, vol. 19, no. 1, pp. 187-199, 1988.
- [35] H. T. Peng, and P. N. Shek, “Novel wound sealants: biomaterials and applications,” *Expert review of medical devices*, vol. 7, no. 5, pp. 639-659, 2010.
- [36] E. Dolgin, “The sticking point,” *Nature medicine*, vol. 19, no. 2, pp. 124-125, 2013.
- [37] R. D. Meyer, S. F. Cogan, T. H. Nguyen *et al.*, “Electrodeposited iridium oxide for neural stimulation and recording electrodes,” *IEEE transactions on neural systems and rehabilitation engineering*, vol. 9, no. 1, pp. 2-11, 2001.

[38] K. Y. Lee, K. H. Bouhadir, and D. J. Mooney, "Degradation Behavior of Covalently Cross-Linked Poly (aldehyde guluronate) Hydrogels," *Macromolecules*, vol. 33, no. 1, pp. 97-101, 2000.

Figure Legends

Fig. 1. Fabrication process of ZnO NW on different substrates. (a-f) Different growth process of ZnO NWs on silicon substrate (g) Similar growth process with optimized growth parameters on the tip of the platinum iridium microwire substrate

Fig. 2 Different growth stages of ZnO NWs. (a) Influence of growth time on ZnO NWs length. (b) SEM images at different growth times (c) ZnO NWs fabricated on tip of microwire with different magnification with optimized growth parameters.

Fig. 3 ZnO NW electrode implantation with sciatic nerve and PEGDA application (a) Electrode base embedded in PEGDA as a substrate to position ZnO NW electrodes (b) ZnO NW electrodes penetrated through the rat sciatic nerve (c) PEGDA applied and cured with UV exposure to maintain fitter contact with neural tissue during stimulation

Fig. 4 Stimulation with ZnO NW electrodes and recording EMG with conventional stainless steel electrodes (a) Raw data with all traces and a mean trace at 60 μ A stimulation current (b) EMG recording at different stimulation current, ranging from 60–160 μ A (c) Variation of EMG peak amplitude with stimulation current (d) Variation of EMG peak time with stimulation current

Fig. 1.

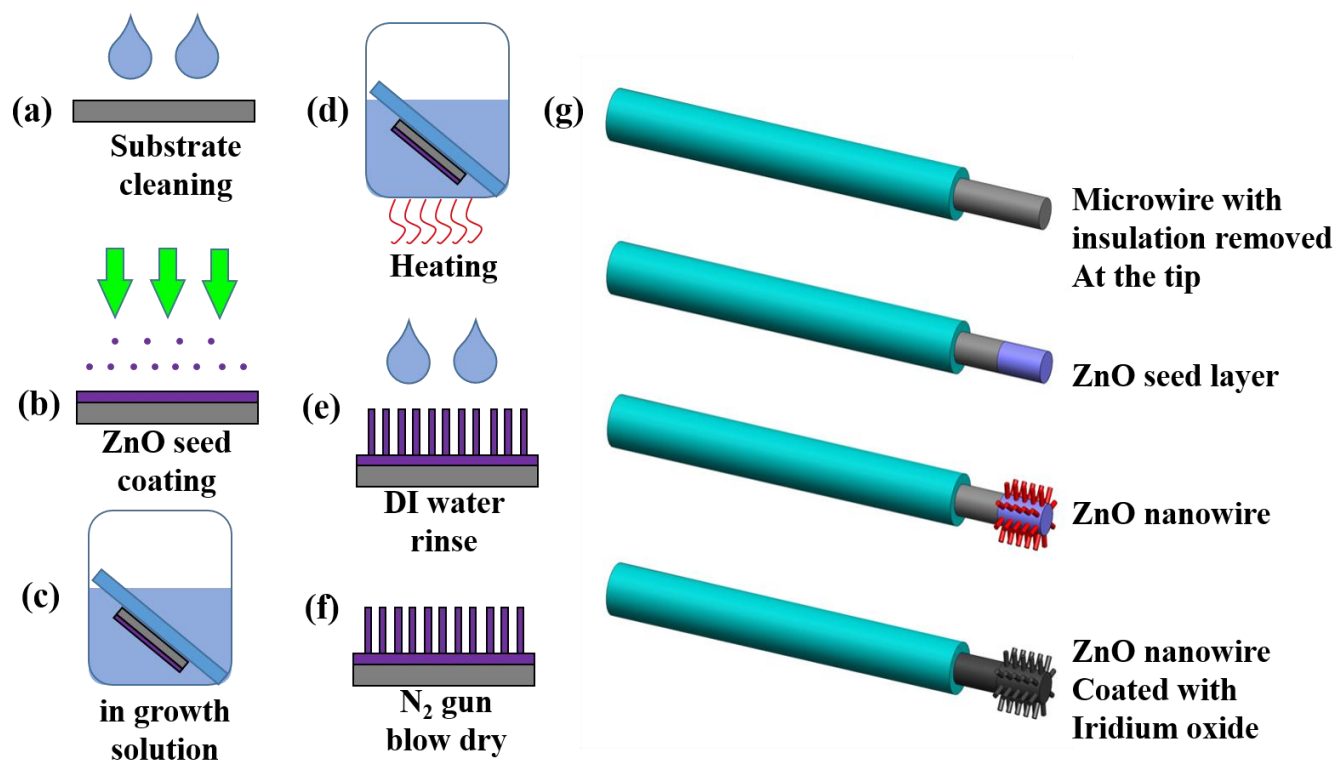


Fig. 2.

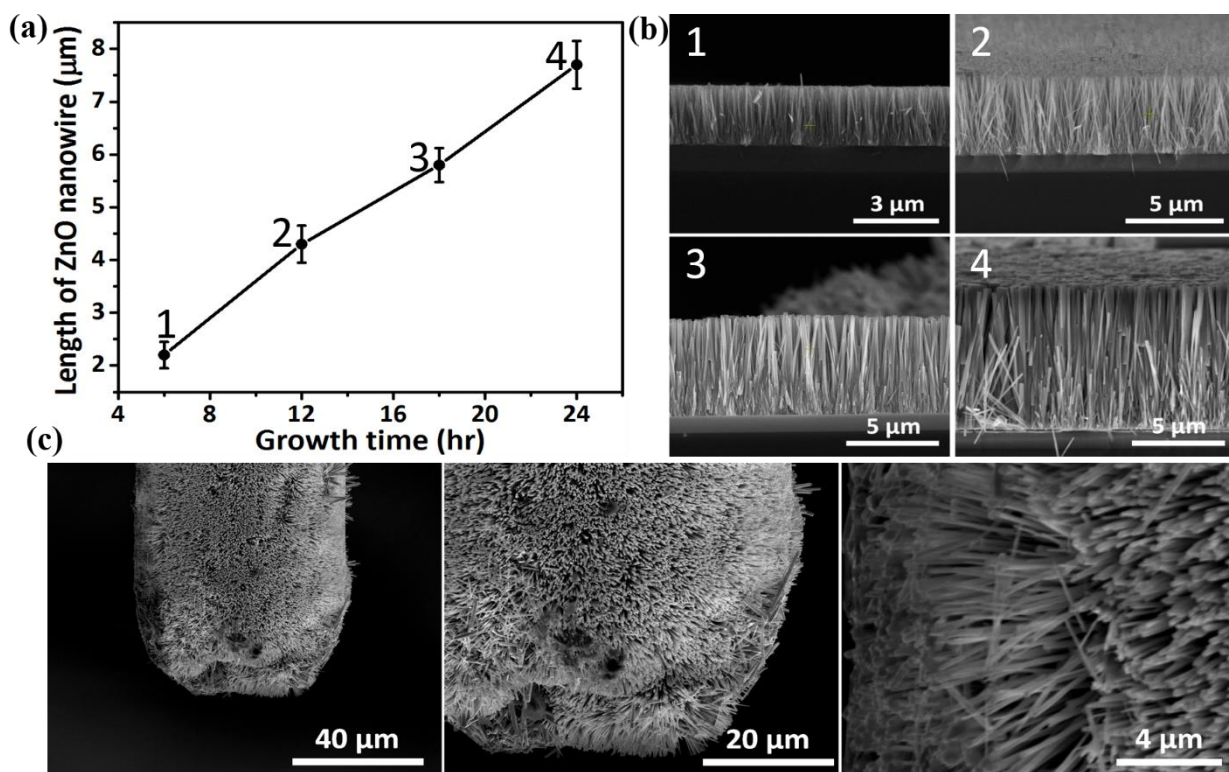


Fig. 3.

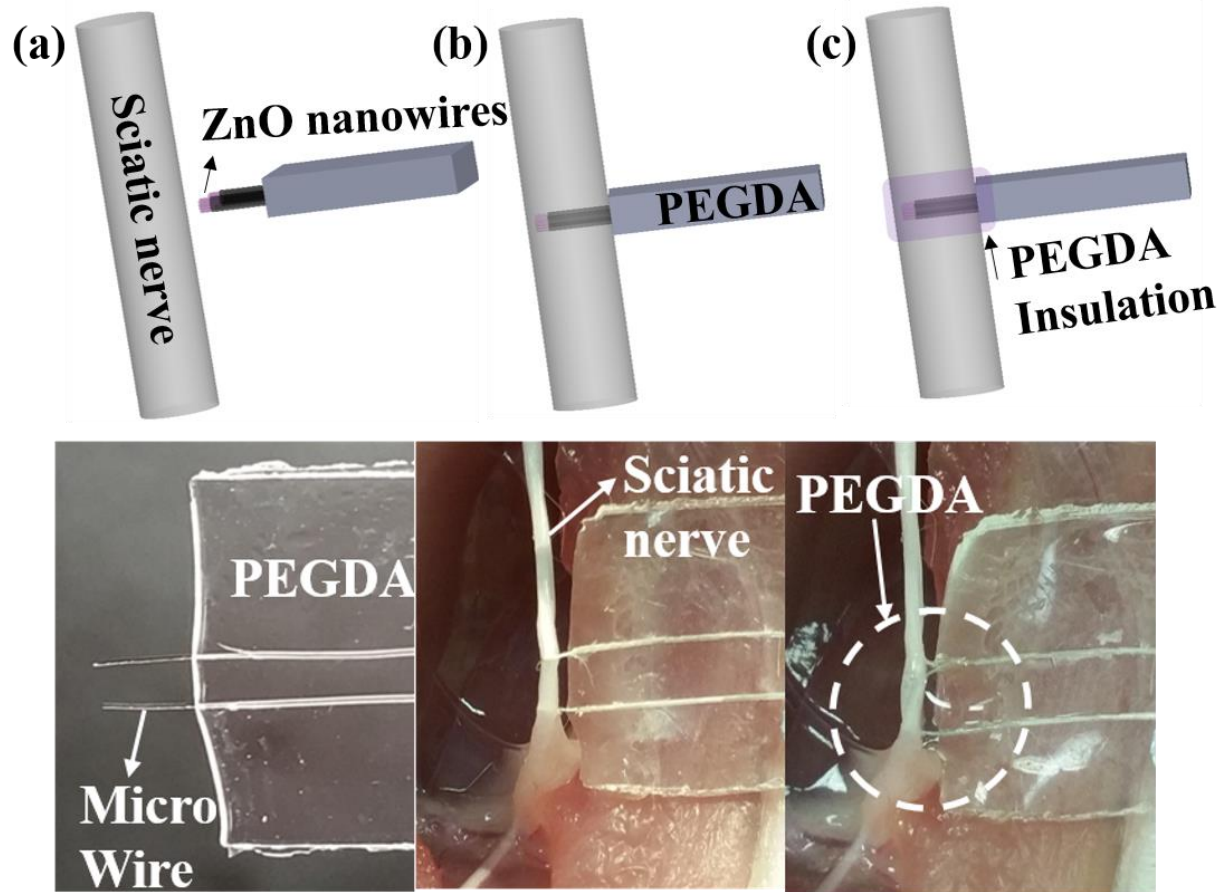


Fig. 4.

